Heliyon 10 (2024) e24860

Contents lists available at ScienceDirect

Heliyon

journal homepage: www.cell.com/heliyon

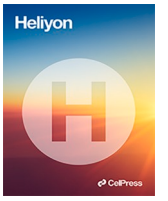

Research article

Significance of N6-methyladenosine RNA methylation regulators in diagnosis and subtype classification of primary Sjögren's syndrome

Jiaoyan Li [a], Kaihong Xie [b], Minxian Xu [b], Ye Wang [c], Yinghong Huang [a], Tao Tan [d,**], Hui Xie [d,e,*]

[a] Department of Rheumatology and Clinical Immunology, The First Hospital of Changsha, Changsha, 410005, Hunan Province, PR China
[b] Department of Oncology, Affiliated Hospital (Clinical College) of Xiangnan University, Chenzhou, 423000, Hunan Province, PR China
[c] Department of Thoracic Surgery, Affiliated Hospital (Clinical College) of Xiangnan University, Chenzhou, 423000, Hunan Province, PR China
[d] Faulty of Applied Sciences, Macao Polytechnic University, Macao, 999078, PR China
[e] Department of Radiation Oncology, Affiliated Hospital (Clinical College) of Xiangnan University, Chenzhou, 423000, Hunan Province, PR China

ARTICLE INFO

Keywords:
N6-methyladenosine
m6A
RNA methylation regulators
Primary Sjögren's syndrome
PSS
Gene expression omnibus database

ABSTRACT

The importance of N6-methyladenine (m6A) in mRNA metabolism, physiology, pathology and other life processes is well recognized. However, the exact role of m6A regulators in primary Sjögren's syndrome (PSS) remains unclear. In this study, we used bioinformatics and machine learning random forest approach to screen eight key m6A regulators from the Gene Expression Omnibus GSE7451, GSE40611 and GSE84844 datasets. An accurate nomogram model for predicting PSS risk was established based on these regulators. And using consensus clustering, patients diagnosed with PSS were classified into two different m6A patterns. We found that patients in group B had higher m6A scores compared to those in group A: furthermore, both groups were closely related to immunity and possibly to other diseases. These results emphasise the important role of m6A regulators in the pathogenesis of PSS. Our study of m6A patterns may inform future immunotherapy strategies for PSS.

1. Introduction

The primary Sjögren's syndrome (PSS) is an autoimmune disease that causes systemic inflammation [1]. The literature reports an incidence rate of approximately 5–7/10,000 individuals, with the highest prevalence observed in European and Asian populations, reaching 43/10,000 individuals [2]. PSS commonly affects exocrine glands, including the lacrimal and salivary glands, resulting in xerostomia and xerophthalmia [3]. PSS can cause significant organ involvement, such as thrombocytopenic purpura, primary biliary cirrhosis, and interstitial pneumonia, that can negatively impact patient outcomes [3]. Despite ongoing research, the pathogenesis of PSS remains incompletely understood, although the prevailing theory suggests that it arises from autoimmune dysregulation [2]. The pathogenesis of PSS, as an autoimmune disease, is very closely related to immunity [4]. Studies have shown that the severity and

* Corresponding author. Department of Radiation Oncology, Affiliated Hospital (Clinical College) of Xiangnan University, No. 25, Renmin West Road, Chenzhou, 423000, Hunan Province, PR China.
** Corresponding author.
E-mail addresses: taotanjs@gmail.com (T. Tan), h.xie@xnu.edu.cn (H. Xie).

https://doi.org/10.1016/j.heliyon.2024.e24860
Received 14 June 2023; Received in revised form 10 January 2024; Accepted 16 January 2024
Available online 23 January 2024

susceptibility of PSS depends on the host's immune response, particularly the size and nature of the immune pathways triggered by pathogen stimuli [3]. It has also been found that patients with PSS exhibit a significantly higher propensity for tumour development due to immunity compared to healthy patients [5]. It is evident that it is feasible to study PSS from an immunological point of view for the purpose of its control. Therefore, the study of genes associated with the initiation of PSS must identify new diagnostic and therapeutic targets. This will help to reduce the incidence of PSS.

N6-methyladenine (m6A) modified eukaryotes are prevalent, participating not only in the entirety of mRNA expression but also in the regulation of other non-coding RNAs, such as transfer RNA, ribosomal RNA, long non-coding RNA, and microRNA [6]. As a result, m6A modification has both extensive and intricate impacts on gene expression regulation. Methyltransferases (Writers), demethylases (Erasers), and m6A-binding proteins (Readers) are mainly involved in the regulatory process [7]. In recent times, an increasing amount of evidence suggests that m6A modification serves as a key regulator in the modulation of immune cell function [6]. Through meRIP-seq analysis, it has been observed that mature dendritic cells exhibit a significant number of genes with m6A modifications in comparison to immature dendritic cells [8]. These genes are primarily associated with the activation of immune and inflammatory responses [8]. A study observed a reduction in viral replication in $CD4^+$ T cells infected with HIV-1 upon the downregulation of METLE3 and METLE14, whereas the upregulation of ALKBH5 led to an increase in viral replication. These results suggest that m6A modifications play a role in T cell immune responses [9]. Additionally, a correlation between the decreased expression of ALKBH5, METLE3, HNRNPC, and KIAA1429 and immune escape in lung squamous cell carcinoma has been established [10]. Increasing data have shown that METTL14 expression is reduced in cervical cancer [11,12], bladder cancer [13] and breast cancer [14], but elevated in thyroid and pancreatic cancers [15], all of which suggest that METTL14 is involved in tumour regulation. A high level of m6A or METTL3 in CRC patients results in a shorter overall survival rate, and METTL3 promotes the progression of the disease [16]. Interestingly, H3K27me3 modulation by m6A negatively regulated the inflammatory response, suggesting a function for m6A in immune homeostasis [17].

Although there is increasing evidence supporting the regulatory role of m6A in the immune response, no reports have yet indicated its potential involvement in the pathogenesis of PSS. Nevertheless, conducting a thorough examination of immune modifications in both healthy and PSS lesion samples, alongside an analysis of PSS subtypes, in conjunction with an exploration of the mechanisms governing m6A regulation in these alterations, has the potential to provide a fresh outlook on advancing our comprehension of the pathogenic mechanism of PSS.

This study presents a comprehensive evaluation of the roles of m6A regulators in the diagnosis of PSS and its subtype classification. For this project, three datasets were used from the Gene Expression Omnibus (GEO): GSE7451, GSE40611, and GSE84844. To predict PSS, a genetic model based on the eight genes of the m6A regulator was developed. The clinical efficacy of this model was found to be favorable for patients. Significantly, the presence of immune cell infiltration and immune responses in PSS exhibited a strong correlation with m6A regulators.It appears that PSS' immune microenvironment is influenced by m6A modification.

2. Materials and methods

2.1. Data collection

The GSE7451 (10 non-PSS and 10 PSS), GSE40611 (18 non-PSS and 31 PSS) and GSE84844 (30 non-PSS and 30 PSS) were obtained from the GEO database (https://www.ncbi.nlm.nih.gov/geo/). R software was used to merge the three datasets. In order to eliminate the variability introduced by the different datasets, the sva package of the R software was used to eliminate the batch effect. We sourced 26 m6A regulators from relevant literature [6,9,18]. Furthermore, 278 m6A-related genes were identified from the m6A2Target database (http://m6a2target.canceromics.org) [10]. The main feature of the site is that a search of the database will then automatically give the genes that are linked to the gene being studied. During the differential expression analysis, using screening criteria of $|\log FC| > 1$, adj.P < 0.05, and FC: Fold Change, we identified 10 m6A regulators (METTL14, WTAP, RBM15, CBLL1, YTHDF1, YTHDF3, HNRNPC, FMR1, IGFBP3, and IGF2BP1) that were differentially expression between normal and PSS tissues.

2.2. Construction of the random forest and support vector machine model

The Random Forest (RF) algorithm employs ensemble learning by integrating multiple decision trees, which is a fundamental component of machine learning. This study utilized the RF algorithm, specifically employing the R software of "RandomForest" and "caret" packages, to identify and assess ten distinctively expressed m6A regulators for their predictive ability in determining the occurrence of PSS. The RF modeling process was conducted with ntrees and mtry set to 500 and 3, respectively [11]. And, to better repeat the experiment, we set the seed to 1234. The significance of the 10 distinct m6A regulators that are differentially expressed in the occurrence of PSS was evaluated through a 10-fold cross-validation process. For the 10-fold cross validation experiment, the number of seeds was also set to 1234, the method was set to CV and number was set to 10. Finally, the results of the experiment are visualized in cross-validation curve. The Y-axis of the cross-validation curve depicted the precision of the model, which was obtained by varying the number of m6A regulators. Support vector machines (SVM), a pattern-recognition method rooted in statistical learning theory, presents numerous benefits in tackling obstacles such as limited sample sizes, nonlinearity, and high-dimensional pattern recognition [12]. In the course of our inquiry, we represented every individual datum as a point within an n-dimensional framework, with n denoting the quantity of m6A regulators involved. SVM is implemented using R software "e1071" and "caret" package. The number of seeds is also set to 1234, and the training and test sets are randomly assigned in the ratio of 2:8. Important genes selected in the test set are evaluated in the SVM model.

The model was constructed using the superior method between RF and SVM, with evaluation metrics including Area Under Curve (AUC), Accuracy, Sensitivity, Positive Predictive Value (PPV), Negative Predictive Value (NPV), and F1 score. The number of true positive (TP), true negative (TN), false positive (FP), and false negative (FN) samples were used to comprehensively evaluate the various metrics and select the optimal algorithm for model construction.

$$Acc = (TP + TN)/(TP + TN + FN) \tag{1}$$

$$Sen = TP/(TP + FN) \tag{2}$$

$$F1 - score = 2TP/(2TP + FN + FP) \tag{3}$$

$$PRV = TP/(TP + FP) \tag{4}$$

$$NPV = TN/(TN + FN) \tag{5}$$

2.3. Constructing prognostic nomogram

Using the "rms" package in the R software, we constructed a Nomogram to forecast the incidence of PSS, relying on the final selection of m6A regulators. Furthermore, a calibration curve was generated in order to assess the degree of agreement between the predicted and observed values. In addition, a decision curve was plotted to further assess the clinical usefulness of the model. The calibration curve and the decision curve were realised through the "rms" and "dca.R" packages of the R software, respectively.

2.4. Identification of molecular subtypes based on m6A regulators

Consensus clustering is a prominent area of investigation in the domain of machine learning and is categorized under unsupervised learning. This technique assesses the suitability of clustering parameters by modifying the clustered dataset and evaluating the consistency of the clustering performance across various samples [13]. Using R software's ConsensusClusterPlus package, a consensus clustering analysis of important m6a regulators was conducted.

3. Gene ontology functional enrichment analysis base on differentially expressed genes between distinct m6A patterns

Based on the binary clustering of m6A using the R software "limma" package, differentially expressed genes (DEGs) were selected based on the $|\log FC| > 1$ and adjusted p-value of 0.05 criteria. In order to visualize the enrichment circle diagram, the "clusterProfile" package in R software was utilized to perform GO enrichment analysis on the screened DEGs.

3.1. Assess of m6A gene signature

The m6A patterns were quantified using the principal component analysis (PCA) technique, which calculated the m6A score for every PSS sample. First, m6A clusters were identified using PCA analysis, then the m6A-score was determined using Formula 6. PCA analysis was implemented through the prcomp(.) function of the R software.

$$m6A - score = PC1i \tag{6}$$

PC1: principal component 1; i: the expression of differential genes.

3.2. Assess of infiltrating immune cells

Single-cell gene set enrichment analysis (ssGSEA) was used to evaluate immune cell infiltration in PSS samples. Within the R, the "GSEA" package was used to conduct the ssGSEA analysis.

3.3. Statistical analysis

The present study investigated the association between writers and erasers through the utilization of a linear regression model. Additionally, Kruskal-Wallis tests were conducted to determine whether groups differed. We conducted all statistical tests as two-tailed tests, with a significant level of adj. $p < 0.05$ considered statistically significant (unless otherwise noted). The statistical analyses were performed using the R softwear.

4. Results

The flow chart of our research is shown in Fig. 1.

4.1. 23 m6A regulators expressed in PSS

Through the use of the R package "limma", a differential expression analysis was conducted on the 23 m6A regulators between non-PSS and PSS cohorts. By screening criteria (|logFC|>1 and adj. $P < 0.05$) 10 m6A regulators showed significant differences (METTL14, WTAP, RBM15, CBLL1, YTHDF1, YTHDF3, HNRNPC, FMR1, IGFBP3, IGF2BP1, as shown in Fig. 2A). From Fig. 2A combined with Fig. 2B, we can find that the expression of the 10 DEGs was significantly higher in METL14,WATP, RBM15, CBLL1, YTHDF3, HNRNPC, HNRNPC, IGFBP3 and significantly lower in YTHDF1 and IGF2BP1 in PSS patients. By using the RCircos package, we were also able to visualize the chromosomal locations of these 23 m6A regulators (in Fig. 2C).

4.2. Detecting the correlation between writers and erasers in PSS patients

The PSS investigated the correlation between writers' expression levels and erasers' expression levels using linear regression analysis. The results of this study demonstrate that expression levels of FTO positive correlation with the expression levels of METTL3 ($r = 0.537$, $p < 0.001$) and ZC3H13 ($r = 0.337$, $p = 0.004$) in the PSS. The same were the expression levels of ALKBH5 positive correlation with the expression levels of METTL3 ($r = 0.234$, $p = 0.050$) and RBM15B ($r = 0.574$, $p < 0.001$).

Conversely, the expression levels of RBM15 ($r = -0.128$, $p = 0.005$), WTAP ($r = -0.348$, $p = 0.003$), and METTL14 ($r = -0.273$, $p = 0.022$) were negatively correlated with the expression levels of ALKBH5 (Fig. 3). These findings suggest that distinct relationships exist between writers and erasers.

4.3. Building the RF and SVM models

To identify m6A modifiers from these 10 differential m6A modifiers that might be used to predict the occurrence of PSS, we built RF

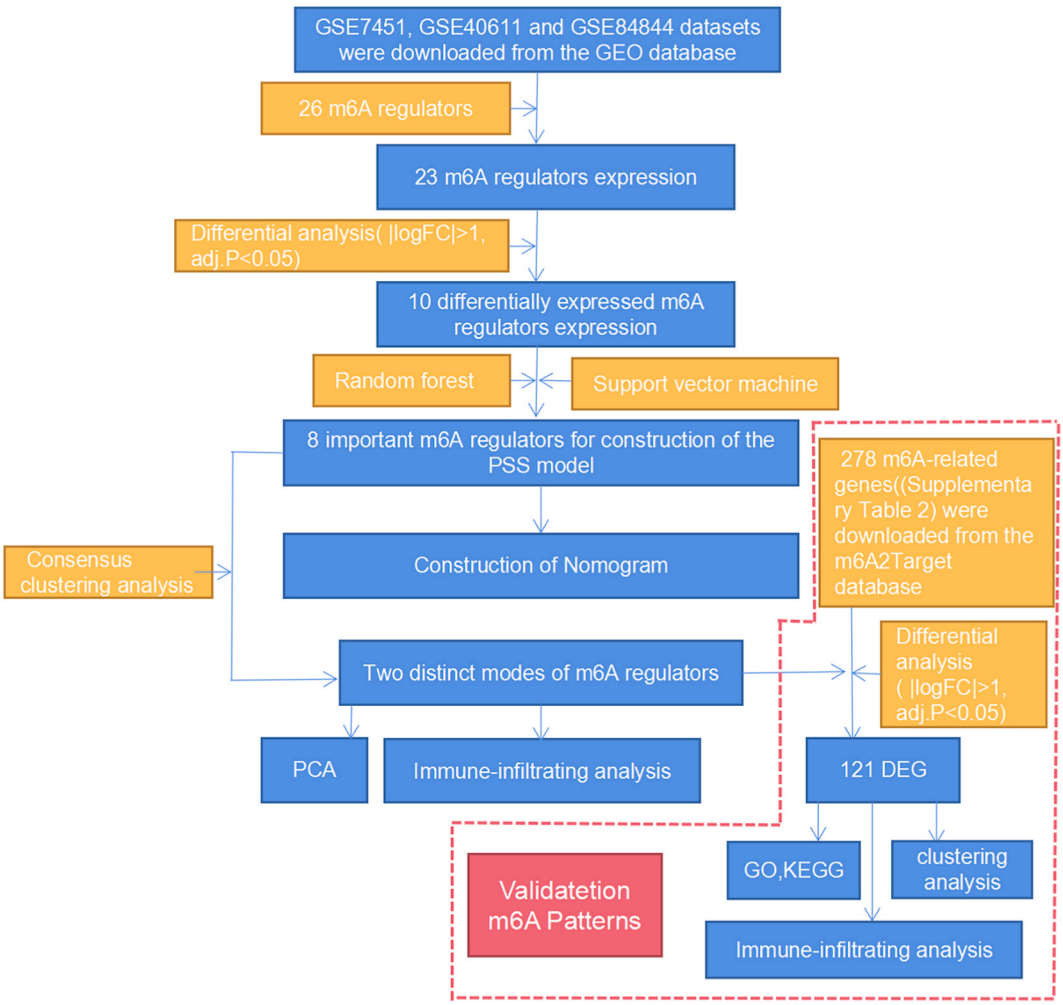

Fig. 1. Technology roadmap of this study.

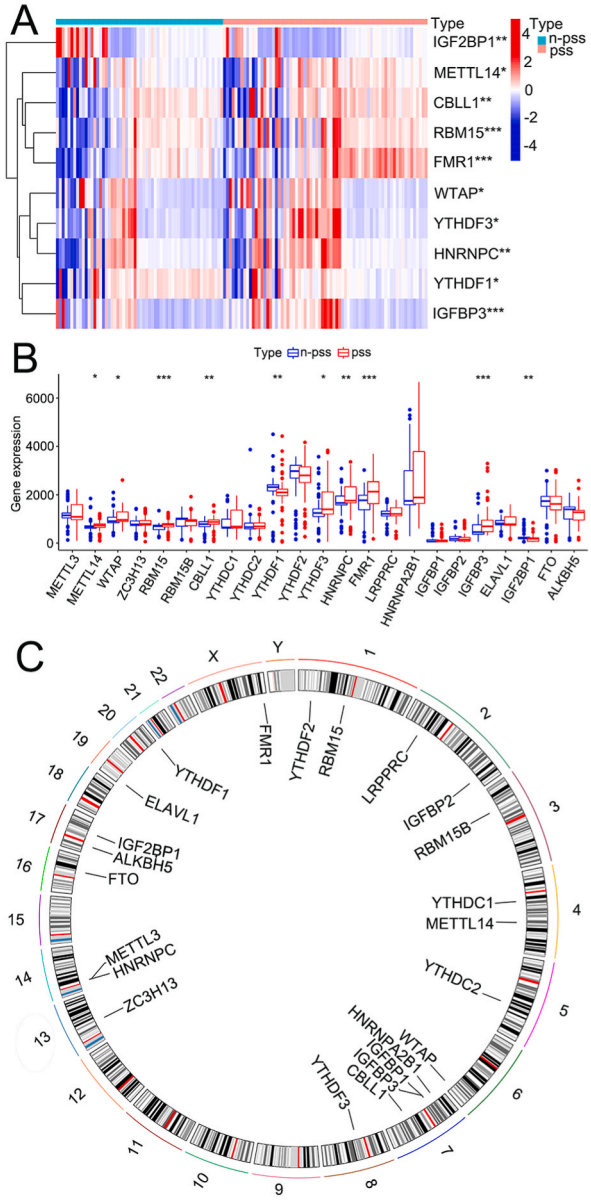

Fig. 2. Expression analysis of m6A regulators in PSS. (A) The heatmap displays of total 10 differentially expressed m6A regulators. (B) The heatmap displays of 23 m6A regulators differences compared with non-PSS and PSS groups, respectively. (C) Chromosomal positions of the 23 m6A regulators. *p < 0.05, **p < 0.01, ***p < 0.001.

and SVM models of PSS. According to the inverse cumulative distribution plot of residuals (Fig. 4A) and the residual box plot (Fig. 4B) and the RF model had the smallest residuals, and many samples of the RF model had lower residuals (Fig. 4B). Based on RF (Fig. 4C), we ranked and visualized candidate m6A regulators to determine their significance in PSS occurrence. The top 8 m6A regulators (YTHDF1, FMR1, IGFBP3, RBM15, YTHDF3, HNRNPC, IGF2BP1, and CBLL1) were selected for model building. The predictive accuracy of the model was evaluated through the plotting of ROC curves. Results indicated that RF had a higher AUC than SVM (Fig. 4D).

RF was used to construct a predictive model for PSS incidence. Randomly, 80% of the dataset was partitioned into a training set and 20% into a validation set. The performance of the RF model was evaluated in both the training and validation sets, as presented in Table 1. We can find that the RF model predicts PSS risk in the training set with AUC (95%CI), accuracy, sensitivity, specificity, PPV, NPV and F1 of 0.909(0.787–1.001), 0.846, 0.818, 0.867, 0.818, 0.867 and 0.818 respectively. The AUC, accuracy, sensitivity, specificity, PPV, NPV and F1 in the validation set were 0.827(0.671–0.984), 0.654, 0.455, 0.800, 0.625, 0.667, 0.526 The results indicate a high level of accuracy in the RF model's predictions. It is also implied that the 8 m6A regulators modelled may play an important role in PSS regulation.

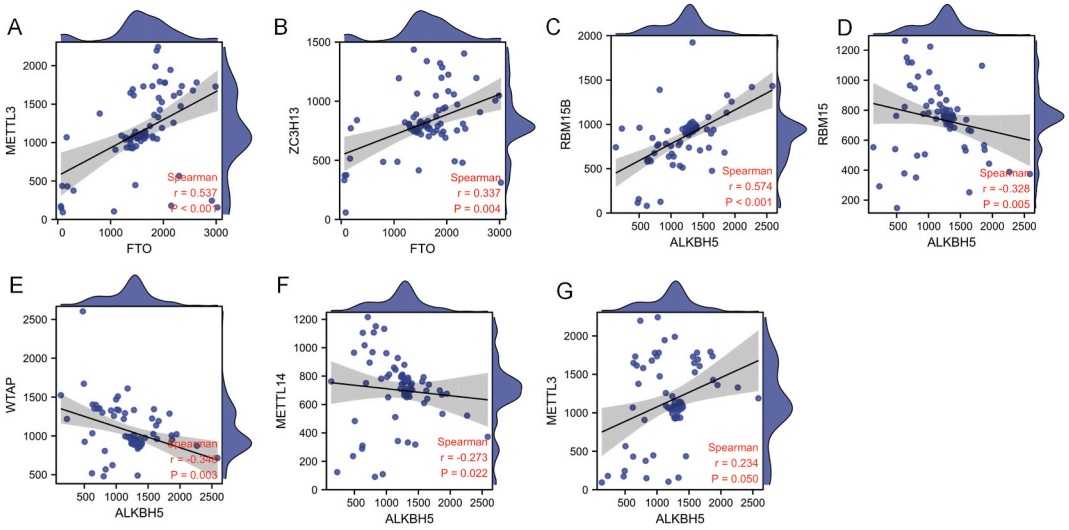

Fig. 3. Pearson correlation revealed significant correlation between writers and erasers in PSS. (A) correlation between METTL3 and FTO, (B) correlation between ZC3H13 and FTO, (C) correlation between RBM15B and ALKBH5, (D) correlation between ALKBH5 and METTL3, (E) correlation between WTAP and ALKBH5, (F) correlation between METTL14 and ALKBH5, (G) correlation between ALKBH5 and METTL15.

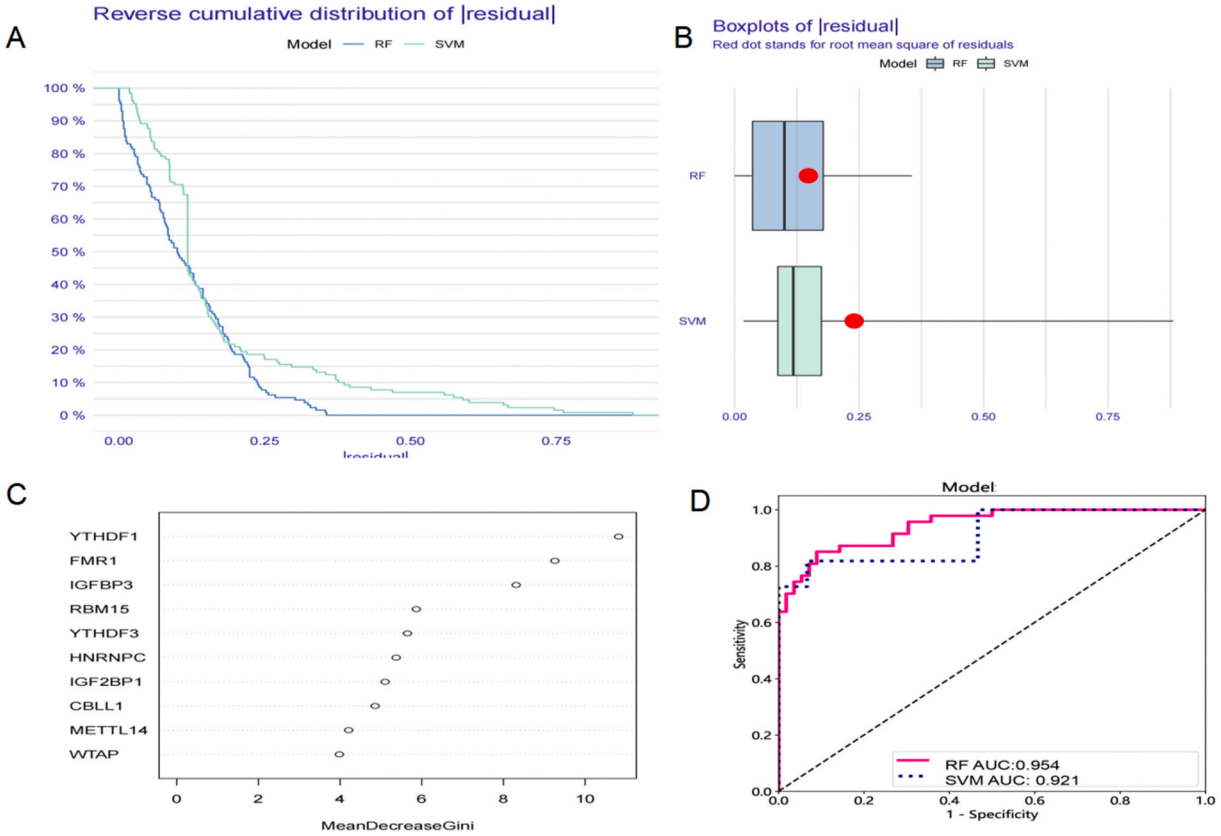

Fig. 4. Random forest model construction. (A) Reverse cumulative distribution curves. (B) The boxplot shows residual distribution. (C) Scaled importance of 9 N6-Methyladenosine RNA methylation regulators in the diagnosis of primary sjögren's syndrome. (D) ROC curves of the prediction models.

Table 1
Summary of evaluation indicators of random forest model in training set and validation set.

	AUC 95%CI	Accuracy	Sensitivity	Specificity	PPV	NPV	F1
Train	0.909(0.787–1.001)	0.846	0.818	0.867	0.818	0.867	0.818
Validation	0.827(0.671–0.984)	0.654	0.455	0.800	0.625	0.667	0.526

Positive Predictive value: PPV; Negative predictive value: NPV.

4.4. Construction of nomogram

With the help of the "rms" package in R software, a nomogram for predicting PSS occurrence was developed based on the 8 core m6A regulators (Fig. 5A). Using this nomogram and 8 hub m6A regulators expression, we can predict the chances of PSS risk very accurately. The calibration curve demonstrated a high degree of concordance between the predicted and actual values (Fig. 5B). It appears that this model is clinically beneficial for PSS patients, based on the DCA curves (Fig. 5C). Further, the clinical impact curve of the model demonstrated its robust predictive capability (Fig. 5D).

4.5. Two distinct modes of m6A regulators

With the help of the R software package ConsensusClusterPlus, a consensus clustering analysis was performed on patients

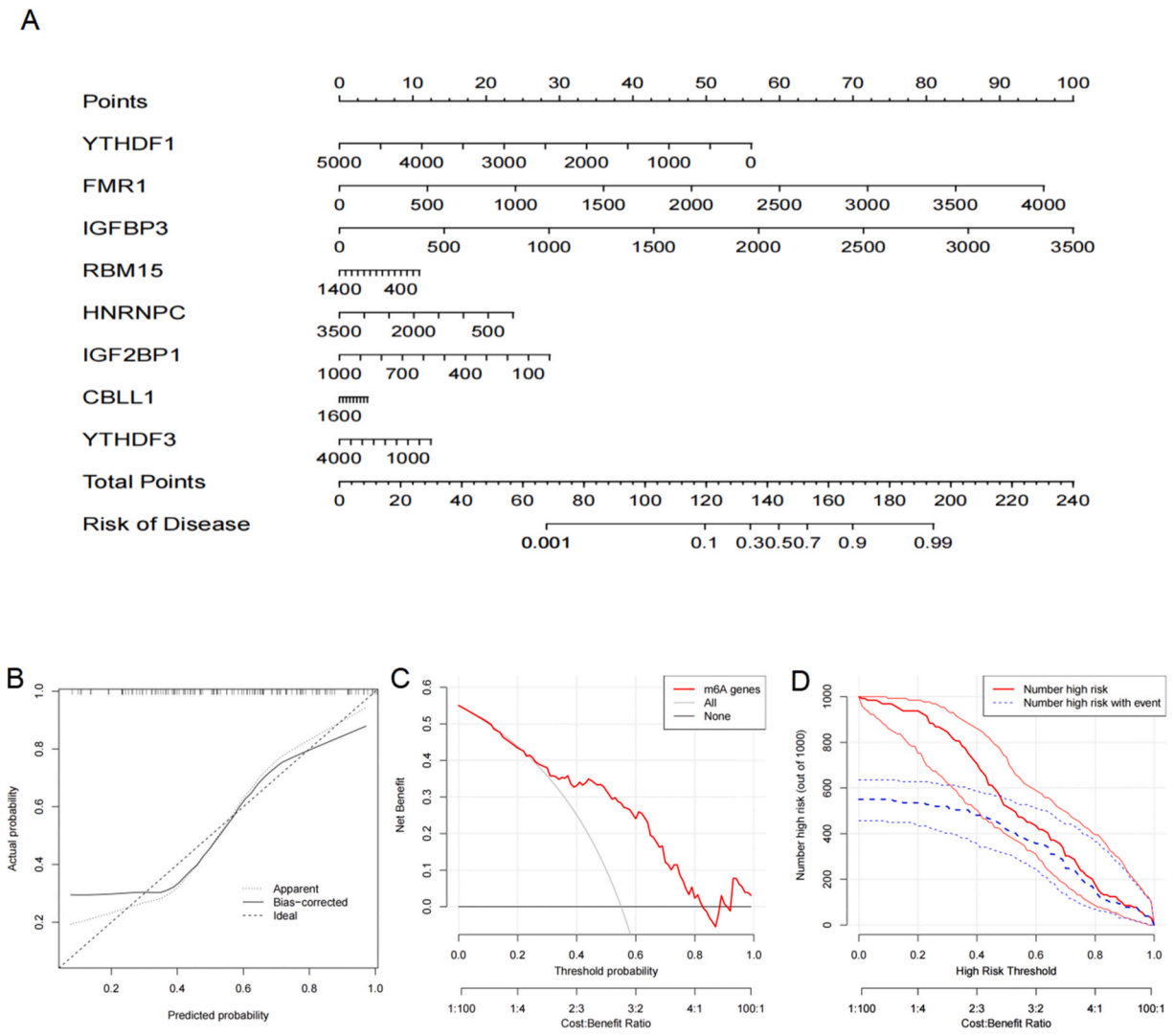

Fig. 5. Construction of nomogram model. (A) Nomogram predicting primary sjögren's syndrome. (B) Calibration characteristics of the nomogram. (C) Decision curve analysis of the nomogram. (D) Clinical impact curve of nomogram model.

diagnosed with PSS. The findings indicate that the most effective approach for classification is to divide the patients into two distinct clusters. Specifically, cluster A comprised 48 PSS patients, while cluster B consisted of 23 PSS patients (Fig. 6A–D). We used heatmaps and histograms to highlight the differences between the two clusters in expression levels of the eight core m6A regulators. The current investigation identified a noteworthy disparity in the levels of expression for YTHDF1, IGFBP3, YTHDF3, HNRNPC, and RBM15 between cluster A and cluster B, with cluster A exhibiting lower expression levels and cluster B displaying higher expression levels. On the other hand, cluster A exhibited higher levels of IGFBP1 expression than cluster B (Supplementary Fig. 1A and B). Nevertheless, the expression levels of CBLL1 and FMR1 did not exhibit any notable disparity between the two clusters (Supplementary Fig. 1A and B). Furthermore, the PCA scatter plot demonstrated that the eight core m6A regulators were capable of completely distinguishing between the two clusters, as depicted in Supplementary Fig. 1C. Differential expression analysis was executed utilizing two clusters of m6A, resulting in the identification of 121 DEGs meeting the criteria of $\log|FC| > 1$ and adj. p-value < 0.05. These DEGs were subsequently subjected to GO enrichment analysis and presented through an enrichment circle diagram (Supplementary Fig. 2). The outcomes of the analysis revealed that GO:0048732, GO: 0048608, GO: 0030667, GO:0005667, GO:0140297, GO:0061629, and GO:0001223 were all associated with cell proliferation and the physiology of glands. The KEGG database revealed that pathways of DEGs were predominantly enriched in certain immune diseases, such as Human papillomavirus infection and human T-cell leukemia virus 1 infection (Supplementary Fig. 3). Subsequently, we utilized ssGSEA to compute immune-infiltrating abundance in PSS samples and evaluated the correlation between immune-infiltrating cells and eight core m6a regulators.

It was observed that FMR1 exhibited a robust positive correlation with nearly all immune-infiltrating cells (as depicted in Fig. 7A). Subsequently, the immune-infiltrating cells were segregated into two cohorts based on their FMR1 expression levels, and differential expression analysis was conducted. The FMR1 high expression group exhibited greater immune-infiltrating cells in comparison to the FMR1 low expression group, with the exception of Type 2 T helper cells, which displayed lower immune-infiltrating cells in the FMR1 high expression group (as illustrated in Supplementary Fig. 4A). Subsequently, an examination was conducted to discern the variances in immune-infiltrating cells between the two m6A clusters, wherein it was discovered that the m6A pattern exhibited a robust correlation with immune-infiltrating cells. Specifically, cluster A was predominantly associated with Th1 dominant immunity, whereas cluster B was linked to Th2 dominant immunity and B cell immunity response, thereby implying that cluster B may be associated with PSS (Supplementary Fig. 4B).

4.6. *Distinct m6A gene patterns and m6A gene signatures*

Based on the m6A-related DEGs, the PSS patients were segregated into two groups (Fig. 8A–D) to enhance the credibility of the m6A

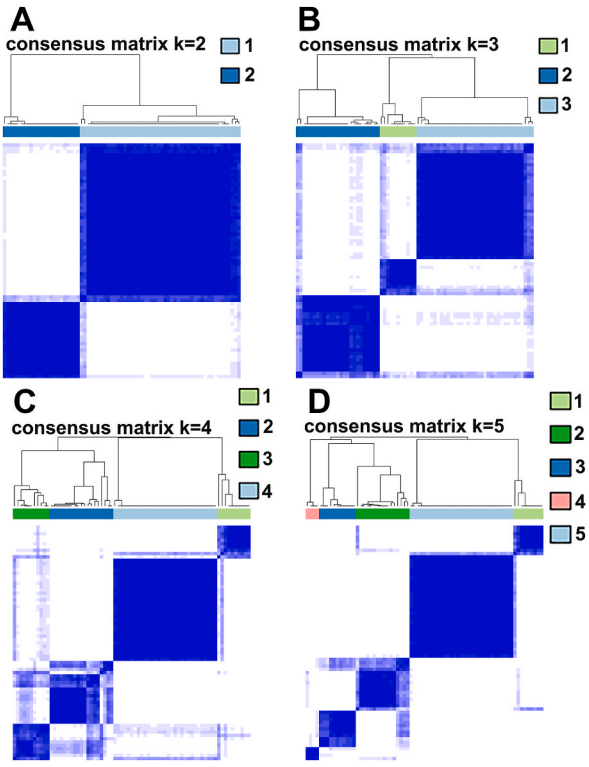

Fig. 6. Determination of optimal number of m6A clusters. The subclusters of primary sjögren's syndrome patients divided by consensus clustering analysis (A) k = 2, (B) k = 3, (C) k = 4, (D) k = 5. Optimal clusters (k = 2) were generated.

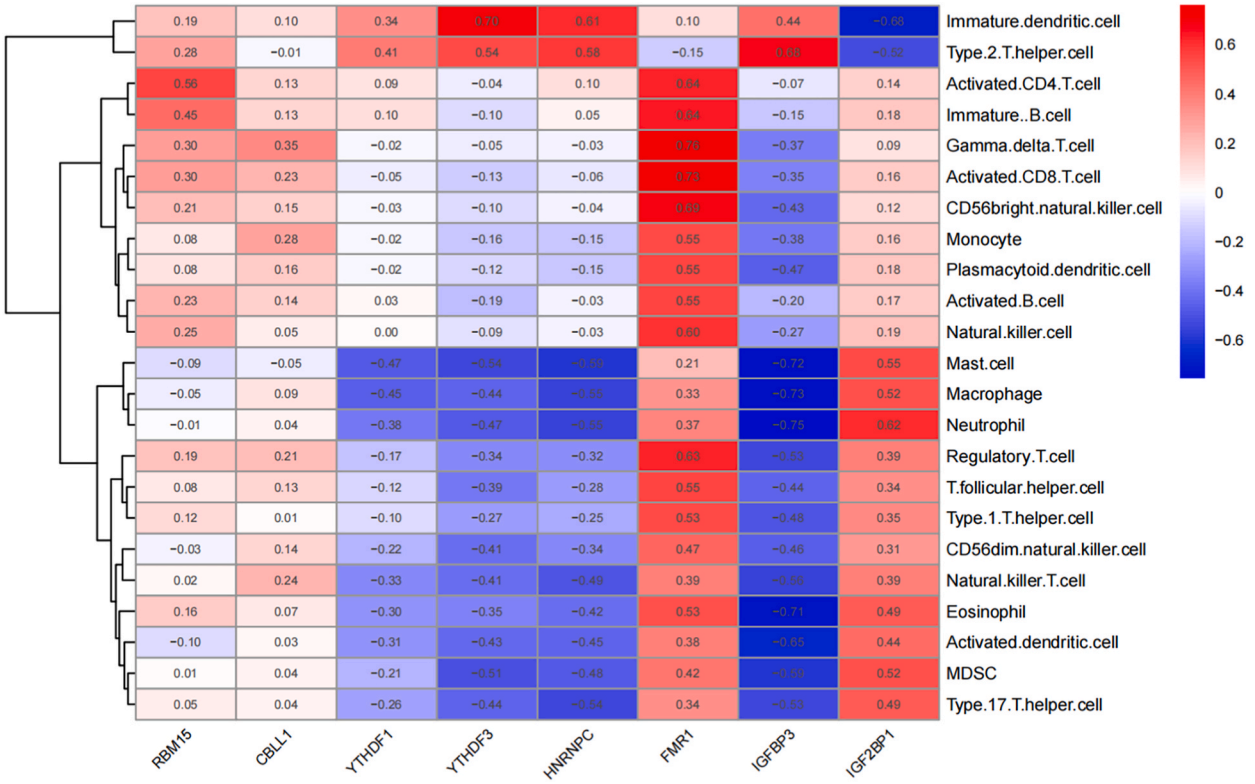

Fig. 7. Correlation between infiltrating immune cells and the 8 significant RNA N6-methyladenosine regulators.

patterns. In Supplementary Fig. 5 and 121 DEGs are shown in gene clusters A and B. Supplementary Figs. 6A and B provide evidence indicating that the expression levels of the eight core m6A regulators, as well as the presence of immune-infiltrating cells, exhibit similarities to the m6A pattern observed between gene cluster A and B. Utilizing consensus clustering, the present study confirms the accuracy of our binary clustering approach. For each sample, we computed the m6A scores using the PCA algorithm. Subsequently, we conducted a comparative analysis of the m6A scores between m6A clusters and m6A gene clusters. As compared with cluster A or gene cluster A, cluster B scores for m6A show a significantly higher increase (Supplementary Fig. 6C and D). To visually depict the relationships between m6A clusters, m6A gene clusters, and m6A scores, we employed a Sankey diagram (Fig. 9A). Sankey diagrams showed higher confidence in Cluster B versus low m6A scores.

4.7. Role of m6A patterns in identification of PSS

To enhance the understanding of the association between m6A patterns and PSS, an inquiry was undertaken to examine the connection between m6A patterns and diverse cytokines, encompassing thymic stromal lymphopoietin (TSLP) (Fig. 9B), interleukin (IL)-33, IL-4, IL-10, and IL-13 (Fig. 9C). The results of our study demonstrate a notable elevation in the expression levels of TSLP, IL-10, and IL-33 within cluster B and gene cluster B, as opposed to cluster A and gene cluster A. These findings suggest a correlation between cluster B and the activation of TH2 immune response and B cell immune response, both of which are recognized as distinctive attributes of PSS.

5. Discussion

PSS is a chronic autoimmune disorder that primarily impacts women in the middle-aged and elderly population [1]. Recent scientific investigations have elucidated the role of m6A regulators in various human biological mechanisms, encompassing immunomodulation [2,3]. However, it remains unclear how m6A regulators contribute to PSS pathogenesis. The present study aims to elucidate the role of m6A regulators in PSS development via immune mechanisms. In order to accomplish this, we screened a total of 23 m6A regulators, identifying 10 with differential expression between PSS and non-PSS groups. The RF method was employed to construct a model for predicting the incidence of PSS. From a pool of 10 candidate m6A regulators, a set of 8 core m6A regulators (namely, YTHDF1, FYTHDF3, FMR1, IGF2BP1, IGFBP3, RBM15, HNRNPC, and CBLL1) was selected to develop the model. A nomogram was created based on these eight core m6A regulators. The DCA curve analysis indicated that the model developed in this study holds potential clinical utility for PSS patients. This indicates that these 8 core m6A regulators have a very important role in PSS.

There were differences in the expression of m6A regulators in the normal and pSS groups. And FTO was positively correlated with

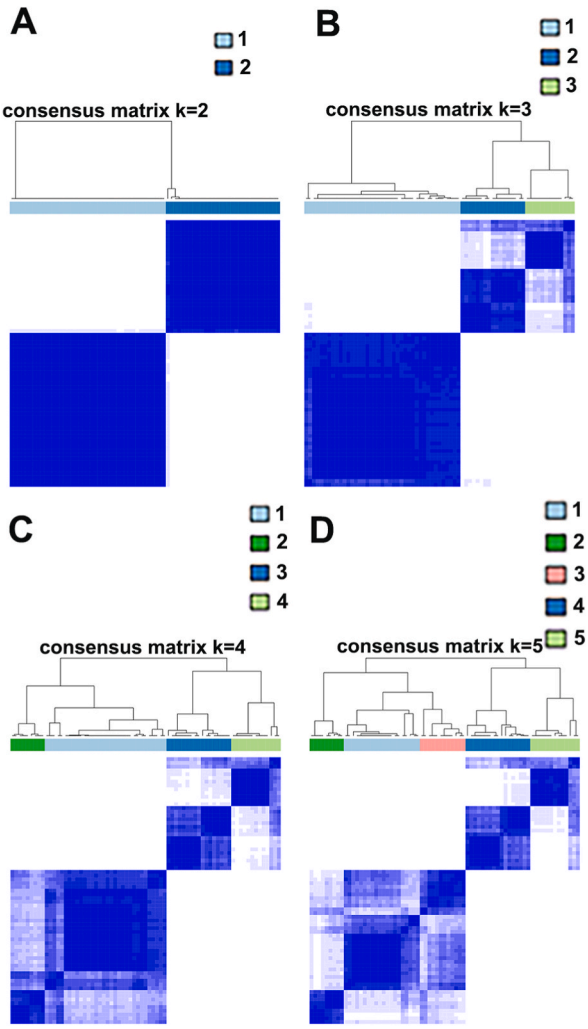

Fig. 8. Determination of optimal number of gene clusters. The subclusters of primary sjögren's syndrome patients divided by consensus clustering analysis (A) k = 2, (B) k = 3, (C) k = 4, (D) k = 5. Optimal clusters (k = 2) were generated.

METTL3 and ZC3H13. ALKBH5 was positively correlated with RBM15B and METTL3, and ALKBH5 was negatively correlated with RBM15, WTAP and METTL14 (Fig. 3). RBM15 is one of 8 core m6A regulators. Effectors such as RBM15 and ALKBH5 can regulate cell cycle biological processes [19]. Overexpression of ALKBH5 resulted in a significant decrease in m6A mRNA levels [20]. ALKBH5 has been implicated in a variety of cancers, viral replication, and metabolic diseases, as well as removing alkylation damage and restoring adenine to DNA [21–23]. RBM15 is an important RNA-binding protein that plays a key role in the biological processes of cells. RBM15 regulates gene expression and RNA processing by binding to RNA molecules, and participates in biological processes such as cell proliferation, differentiation, DNA damage repair, transcriptional regulation, RNA splicing, and translational regulation [24,25]. There is no direct evidence for a direct link between them. However, based on existing studies, it can be speculated that their interaction may involve the regulation of RNA metabolism and gene expression. ALKBH5, as an RNA demethylase, can affect mRNA export and metabolism [22], whereas RBM15, as an RNA-binding protein, can regulate gene expression and RNA processing [24]. Thus, the interaction of ALKBH5 and RBM15 may co-regulate RNA metabolism and gene expression [26]. Thus, the negative correlation between the erased ALKBH5 gene and the authors' RBM15 gene in this study suggests that erasure of ALKBH5 may have a potential relevance in the interaction of RBM15 on PSS.

Cluster analysis showed that different m6A modification patterns had differential gene expression, where YTHDF1, YTHDF3, IGFBP3, IGF2BP1, RBM15 and HNRNPC differed between m6A clusters A and B. Differences between gene clusters A and B are YTHDF3, HNRNPC, FMR1, IGFBP3, IGF2BP1. This suggests that YTHDF3, HNRNPC, IGFBP3 and IGF2BP1 are the key differentiating genes between different m6A modification modes of PSS. According to Shi et al. [27], YTHDF3 has the ability to collaborate with YTHDF1 and YTHDF2 in order to regulate both protein translation and mRNA degradation. Kastan et al. [28] have demonstrated that YTHDF3 can interact with protein translation initiation factors and RBPs, suggesting that YTHDF3 may be involved in the regulation of antiviral innate immune responses at the translational level. YTHDF3 belongs to the TYH family, which includes YTHDF1 and YTHDF3

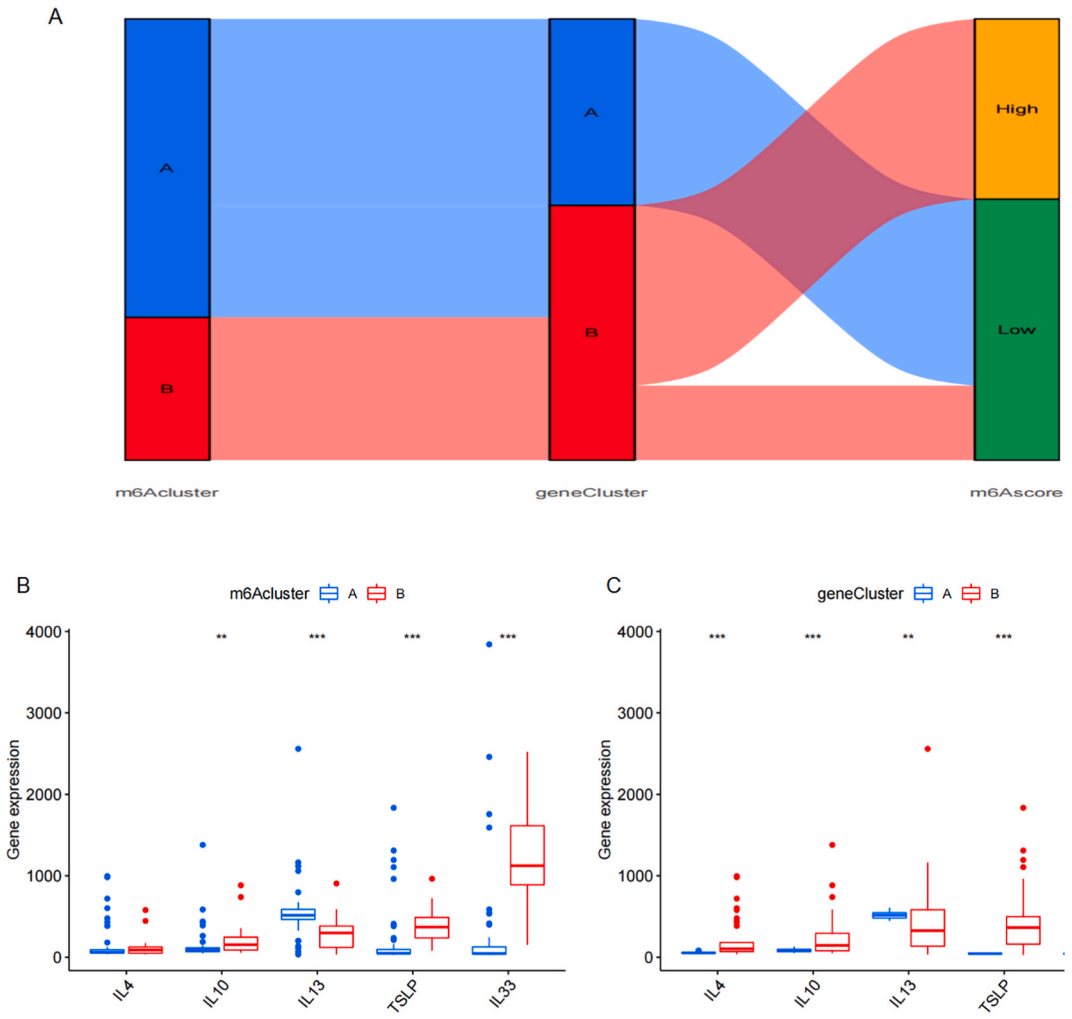

Fig. 9. Role of N6-methyladenosine RNA methylation patterns in distinguishing PSS. (A) Sankey diagram showing the relationship between m6A patterns, m6A gene patterns, and m6A scores. (B) Differential expression levels of thymic stromal lymphopoietin (TSLP), interleukin (IL)-33, IL-4, IL-10, and IL-13 between cluster A and clusterB. (C) Differential expression levels of TSLP, IL-33, IL-4, IL-10, and IL-13 between gene clusterA and gene clusterB. *$p < 0.05$, **$p < 0.01$, and ***$p < 0.001$.

[27]. YTHDF3 and YTHDF1 are both m6A readers [29]. In general, YTHDF3 forms a complex with YTHDF1 to promote transcription, while it forms another complex with YTHDF2 to degrade mRNAs with m6A modifications [30]. Results from our study indicate that the YTHDF3/YTHDF1 complex greatly improves the translation of PSS mRNA. This is similar to the study by Su et al. [31]. Xue et al. [32] have successfully identified IGF2BP1 as a conserved single-stranded RNA-binding protein, which involved in gene expression regulation and is associated with the onset and progression of inflammation. IGF2BP1 has been identified to play important roles in regulating mRNA targets, such as PTEN, ACTB, MAPK4, c-MYC, and CD44, in an m6A-dependent manner [33,34].Transcriptomic studies in the TCGA database have shown that IGF2BP1 mRNA expression is highly increased in a variety of malignant tumours compared to normal tissues, especially in hepatocellular carcinoma (LIHC) tissues, and furthermore, IGF2BP1 expression is positively correlated with advanced tumour stage [35]. Additionally, IGFBP3 plays a role in the modulation of cell proliferation by primarily inducing apoptosis to impede cell proliferation [36]. IGFBP3 plays a role in the regulation of cellular proliferation by primarily inducing apoptosis to impede such proliferation. This is potentially achieved through the IGFBP3 membrane receptor's hindrance of the IGF1R pathway, activation of the Smad2/Smad or STAT1 pathway, and nuclear aggregation of IGFBP3 [37,38] IGFBP3 is implicated in the antiproliferative effects mediated by cytokines [36]. Research has demonstrated that FMR1 can present vitamin B2 metabolites of bacterial and fungal origin as antigens [39], thereby facilitating the elimination of infected cells by FMR1-restricted T cells. Additionally, FMR1 has been shown to activate MAIT cells, which in turn prevent the active targeting of viruses and cancer cells by T-cells and NK-cells [40]. As a result of its association with the m6A methylation switch, HNRNPC indirectly controls target gene expression [41], thereby exerting an anti-regulatory effect on the immune system and affecting various biological activities. Wu et al. have reported that the knockdown of HNRNPC can activate the production of type I interferon in tumor cells, leading to a robust intracellular immune response that significantly inhibits cell proliferation and tumor growth [42].

In immune infiltration analyses, each modification pattern also had its own unique immunoprofile. Correlation analysis of immune cells and genes showed that YTHDF1, YTHDF3, HNRNPC and IGFBP3 were negatively correlated with a range of immune cells in PSS samples. While RBM15, CBLL1, FMR1 and IGF2BP1 were positively correlated with a range of immune cells. This implies that m6A regulators is closely related to immunity. Therefore it is feasible to find new targets for treating immune diseases through m6A regulators. It was shown that the initiation of T-cell immune responses was enhanced in YTHDF1-deficient mice with stronger anti-tumour $CD8^+$ T-cell responses [43]. In colon cancer, knockdown of YTHDF1 enhances PD-L1 immunotherapy [44]. It has also been shown that knockdown of YTHDF3 significantly reduced the migration and invasion ability of TNBC cells [45].

The results of the analysis of the differential genes KEGG and GO in the two m6A modification patterns revealed that the pathways were mostly for various types of tumours and a number of diseases:Breast cancer, Pancreatic cancer, Chronic myeloid leukemia, AGE-RAGE signaling pathway in diabetic complications.This suggests that PSS is closely related to the development of various types of tumours and some diseases. The m6A writer METTL3 has oncogenic [46] and tumour suppressor [47]functions in glioblastomas. Wang et al. [48] found that m6A proteins affect tumour proliferation and metastasis in breast cancer and are strongly associated with patient prognosis. Cao et al. [49] demonstrated the regulatory role of m 6 A methylation in the tumour immune microenvironment (TIME). These studies suggest that PSS as well as some malignant diseases can be treated by targeting m6A mRNA methylation.

In this study, we found a complex correlation between m6Acluster, m6A.gene.cluster, m6A scores, and the stages of PSS development, which is well demonstrated in the for Sankey diagram. This complexity of may be determined with the disease specificity of PSS. Currently, the majority of research indicates that PSS is an autoimmune disorder that is intricately linked to the anomalous activation and proliferation of B cells [50]. Overexpression of BAFF triggers aberrant activation of B cells, which subsequently differentiate into plasma cells, resulting in the production of large amounts of autoantibodies and immune complexes [51].BAFF expression is regulated by the cytokines IFN-α, IFN-β, LPS, IL-10, and IL-4, among others [52,53]. Th1 cells mainly produce IL12, IFN-γ and TNF, whereas Th2 cells mainly produce IL-4, IL-5 and IL-10 [54]. The critical role of cytokine pairs on Th1/Th2 balance in regulating BAFF expression [55]. It has been found that ILC2 activation by IL-33 and TSLP directly stimulates Th2 cytokines as well as IL-13, IL-5, IL-4, and IL-9 [56]. IL-4 plays a key role in driving the differentiation of Th0 cells to Th2 cells, while exerting a potent inhibitory effect on Th1 cells [57]. In addition, IL13 is also a key factor in promoting Th2 cell differentiation [57]. In addition, IL10 has been observed to exhibit dual inhibitory effects on Th1 and Th2 cells through different pathways [58]. Our study employed a consensus clustering method to identify two m6A clusters on the PSS, utilizing 8 core m6A regulators. Cluster B exhibited a strong correlation with the immune response to Th2. Notably, the expression levels of IL10, IL-33, and TSLP were significantly elevated in cluster B, indicating a potential association with PSS. Furthermore, the clustering approach based on m6A-related differential genes provided additional support for the validity of our findings. Upon completion of the study, the quantification of m6A clustering patterns was achieved through the utilization of the PCA algorithm, resulting in the calculation of m6A scores for each sample. The findings indicated that both m6A cluster B and gene cluster B exhibited higher m6A scores in comparison to m6A cluster A or gene cluster A.

However, there are some shortcomings in this study that need to be clarified. The results are based on bioinformatics analyses; many of them are theoretical and have not been experimentally verified. Therefore their accuracy needs to be improved and further experiments are needed to support them. However, in this study, combining the consistent results of several bioinformatics analyses and a review of the relevant literature. We believe that these computational predictions can provide valuable references for understanding the m6A-related mechanisms regulating the development of pSS. However, experiments are the best criterion to verify hypotheses, so in the future we will further validate the experiments through experiments.

6. Conclusions

In conclusion, the present study used a screening process to identify eight basic m6A regulators and constructed a nomogram model that showed high accuracy in predicting the incidence of PSS. In addition, the present study identified two different m6A patterns using the above eight core m6A regulators, of which group B may be associated with PSS and also influence the occurrence of other malignant diseases. In addition, we found that m6A regulators interact with immune mechanisms to directly influence the development of PSS. These findings may help to develop potential therapeutic strategies for PSS.

7. Impact statement

Currently, we are investigating whether N6-Methyladenosine RNA methylation regulators play a role in diagnosing and classifying primary Sjögren's Syndrome subtypes. To achieve this objective, a bioinformatics approach was employed to screen eight crucial m6A regulators from the Gene Expression Omnibus GSE7451, GSE40611, and GSE84844 datasets, using the machine learning random forest method. Subsequently, a novel nomogram model was developed based on these eight m6A regulators to predict the risk of PSS. Nomogram model could be beneficial for patients, according to the results of decision curve analysis. It appears that m6A regulators may play a crucial role in the pathogenesis of PSS. Future immunotherapy strategies may be informed by our study of m6A patterns.

Funding

This study was supported by:

1. Key Laboratory of Tumor Precision Medicine, Hunan Colleges and Universities Project (2019-379).
2. A Project Supported by Scientific Research Fund of Hunan Provincial Education Department (20k118).

3. Science and Technology Development Fund of Macao (0041/2023/RIB2).
4. Macao Polytechnic University Grant (RP/FCA-05/2022).

Data availability

The datasets used and/or analysed during the current study available from the corresponding author on reasonable request.

CRediT authorship contribution statement

Jiaoyan Li: Writing – original draft. **Kaihong Xie:** Data curation. **Minxian Xu:** Data curation. **Ye Wang:** Data curation. **Yinghong Huang:** Data curation. **Tao Tan:** Writing – review & editing. **Hui Xie:** Writing – review & editing.

Declaration of competing interest

The authors declare that they have no known competing financial interests or personal relationships that could have appeared to influence the work reported in this paper.

Appendix A. Supplementary data

Supplementary data to this article can be found online at https://doi.org/10.1016/j.heliyon.2024.e24860.

References

[1] G.E. Thorlacius, A. Björk, M. Wahren-Herlenius, Genetics and epigenetics of primary Sjögren syndrome: implications for future therapies, Nat. Rev. Rheumatol. 19 (5) (2023 May) 288–306, https://doi.org/10.1038/s41584-023-00932-6. Epub 2023 Mar 13. PMID: 36914790; PMCID: PMC10010657.
[2] Q. Pilson, S. Smith, C.A. Jefferies, J Ng-D, C.C. Murphy, miR-744-5p contributes to ocular inflammation in patients with primary Sjogrens Syndrome, Sci. Rep. 10 (1) (2020) 7484, https://doi.org/10.1038/s41598-020-64422-5.
[3] P. Soret, C. Le Dantec, E. Desvaux, N. Foulquier, B. Chassagnol, S. Hubert, C. Jamin, G. Barturen, G. Desachy, V. Devauchelle-Pensec, C. Boudjeniba, D. Cornec, A. Saraux, S. Jousse-Joulin, N. Barbarroja, I. Rodríguez-Pintó, E. De Langhe, L. Beretta, C. Chizzolini, L. Kovács, T. Witte, Precisesads Clinical Consortium, Precisesads Flow Cytometry Consortium, E. Bettacchioli, A. Buttgereit, Z. Makowska, R. Lesche, M.O. Borghi, J. Martin, S. Courtade-Gaiani, L. Xuereb, M. Guedj, P. Moingeon, M.E. Alarcón-Riquelme, L. Laigle, J.O. Pers, A new molecular classification to drive precision treatment strategies in primary Sjögren's syndrome, Nat. Commun. 12 (1) (2021 Jun 10) 3523, https://doi.org/10.1038/s41467-021-23472-7. PMID: 34112769; PMCID: PMC8192578.
[4] J. Tarn, D. Lendrem, P. McMeekin, C. Lendrem, B. Hargreaves, W.F. Ng, Primary Sjögren's syndrome: longitudinal real-world, observational data on health-related quality of life, J. Intern. Med. 291 (6) (2022 Jun) 849–855, https://doi.org/10.1111/joim.13451. Epub 2022 Jan 24. PMID: 35018685; PMCID: PMC9305875.
[5] P. Soret, C. Le Dantec, E. Desvaux, N. Foulquier, B. Chassagnol, S. Hubert, C. Jamin, G. Barturen, G. Desachy, V. Devauchelle-Pensec, C. Boudjeniba, D. Cornec, A. Saraux, S. Jousse-Joulin, N. Barbarroja, I. Rodríguez-Pintó, E. De Langhe, L. Beretta, C. Chizzolini, L. Kovács, T. Witte, Precisesads Clinical Consortium, Precisesads Flow Cytometry Consortium, E. Bettacchioli, A. Buttgereit, Z. Makowska, R. Lesche, M.O. Borghi, J. Martin, S. Courtade-Gaiani, L. Xuereb, M. Guedj, P. Moingeon, M.E. Alarcón-Riquelme, L. Laigle, J.O. Pers, A new molecular classification to drive precision treatment strategies in primary Sjögren's syndrome, Nat. Commun. 12 (1) (2021 Jun 10) 3523, https://doi.org/10.1038/s41467-021-23472-7. PMID: 34112769; PMCID: PMC8192578.
[6] Z. Zhang, K. Luo, Z. Zou, M. Qiu, J. Tian, L. Sieh, H. Shi, Y. Zou, G. Wang, J. Morrison, A.C. Zhu, M. Qiao, Z. Li, M. Stephens, X. He, C. He, Genetic analyses support the contribution of mRNA N(6)-methyladenosine (m(6)A) modification to human disease heritability, Nat. Genet. 52 (9) (2020) 939–949, https://doi.org/10.1038/s41588-020-0644-z.
[7] Y. Chen, Y. Zhao, J. Chen, C. Peng, Y. Zhang, R. Tong, Q. Cheng, B. Yang, X. Feng, Y. Lu, H. Xie, L. Zhou, J. Wu, S. Zheng, ALKBH5 suppresses malignancy of hepatocellular carcinoma via m6A-guided epigenetic inhibition of LYPD1, Mol. Cancer 19 (1) (2020 Aug 10) 123, https://doi.org/10.1186/s12943-020-01239-w. PMID: 32772918; PMCID: PMC7416417.
[8] H.N. Fan, Z.Y. Chen, X.Y. Chen, M. Chen, Y.C. Yi, J.S. Zhu, J. Zhang, METTL14-mediated m6A modification of circORC5 suppresses gastric cancer progression by regulating miR-30c-2-3p/AKT1S1 axis, Mol. Cancer 21 (1) (2022 Feb 14) 51, https://doi.org/10.1186/s12943-022-01521-z. PMID: 35164771; PMCID: PMC8842906.
[9] C. Gu, Z. Wang, N. Zhou, G. Li, Y. Kou, Y. Luo, Y. Wang, J. Yang, F. Tian, Mettl14 inhibits bladder TIC self-renewal and bladder tumorigenesis through N(6)-methyladenosine of Notch1, Mol. Cancer 18 (1) (2019) 168, https://doi.org/10.1186/s12943-019-1084-1.
[10] S. Deng, H. Zhang, K. Zhu, X. Li, Y. Ye, R. Li, X. Liu, D. Lin, Z. Zuo, J. Zheng, M6A2Target: a comprehensive database for targets of m6A writers, erasers and readers, Briefings Bioinf. 22 (3) (2021), https://doi.org/10.1093/bib/bbaa055.
[11] X. Chen, M. Xu, X. Xu, K. Zeng, X. Liu, B. Pan, C. Li, L. Sun, J. Qin, T. Xu, B. He, Y. Pan, H. Sun, S. Wang, METTL14-mediated N6-methyladenosine modification of SOX4 mRNA inhibits tumor metastasis in colorectal cancer, Mol. Cancer 19 (1) (2020) 106, https://doi.org/10.1186/s12943-020-01220-7.
[12] X. Yang, S. Zhang, C. He, P. Xue, L. Zhang, Z. He, L. Zang, B. Feng, J. Sun, M. Zheng, METTL14 suppresses proliferation and metastasis of colorectal cancer by down-regulating oncogenic long non-coding RNA XIST, Mol. Cancer 19 (1) (2020) 46, https://doi.org/10.1186/s12943-020-1146-4.
[13] C. Guimarães-Teixeira, J. Lobo, V. Miranda-Gonçalves, D. Barros-Silva, C. Martins-Lima, S. Monteiro-Reis, J.P. Sequeira, I. Carneiro, M.P. Correia, R. Henrique, C. Jerónimo, Downregulation of m6 A writer complex member METTL14 in bladder urothelial carcinoma suppresses tumor aggressiveness, Mol. Oncol. 16 (9) (2022 May) 1841–1856, https://doi.org/10.1002/1878-0261.13181. Epub 2022 Mar 24. PMID: 35048498; PMCID: PMC9067151.
[14] P.J. Gong, Y.C. Shao, Y. Yang, W.J. Song, X. He, Y.F. Zeng, S.R. Huang, L. Wei, J.W. Zhang, Analysis of N6-methyladenosine methyltransferase reveals METTL14 and ZC3H13 as tumor suppressor genes in breast cancer, Front. Oncol. 10 (2020) 578963, https://doi.org/10.3389/fonc.2020.578963.
[15] M. Wang, J. Liu, Y. Zhao, R. He, X. Xu, X. Guo, X. Li, S. Xu, J. Miao, J. Guo, et al., Upregulation of METTL14 mediates the elevation of PERP mRNA N6 adenosine methylation promoting the growth and metastasis of pancreatic cancer, Mol. Cancer 19 (1) (2020) 130, https://doi.org/10.1186/s12943-020-01249-8.
[16] J. Pan, F. Liu, X. Xiao, R. Xu, L. Dai, M. Zhu, H. Xu, Y. Xu, A. Zhao, W. Zhou, Y. Dang, G. Ji, METTL3 promotes colorectal carcinoma progression by regulating the m6A-CRB3-Hippo axis, J. Exp. Clin. Cancer Res. 41 (1) (2022 Jan 10) 19, https://doi.org/10.1186/s13046-021-02227-8. PMID: 35012593; PMCID: PMC8744223.
[17] C. Wu, W. Chen, J. He, S. Jin, Y. Liu, Y. Yi, Z. Gao, J. Yang, J. Yang, J. Cui, W. Zhao, Interplay of m6A and H3K27 trimethylation restrains inflammation during bacterial infection, Sci. Adv. 6 (34) (2020 Aug 19) eaba0647, https://doi.org/10.1126/sciadv.aba0647. PMID: 32875102; PMCID: PMC7438091.

[18] I.A. Roundtree, M.E. Evans, T. Pan, C. He, Dynamic RNA modifications in gene expression regulation, Cell 169 (7) (2017) 1187–1200, https://doi.org/10.1016/j.cell.2017.05.045.

[19] C. Zhang, M. Zhang, S. Ge, et al., Reduced m6A modification predicts malignant phenotypes and augmented Wnt/PI3K-Akt signaling in gastric cancer, Cancer Med. 8 (2019) 4766–4781.

[20] Y. Yuan, G. Yan, M. He, H. Lei, L. Li, Y. Wang, X. He, G. Li, Q. Wang, Y. Gao, Z. Qu, Z. Mei, Z. Shen, J. Pu, A. Wang, W. Zhao, H. Jiang, W. Du, L. Yang, ALKBH5 suppresses tumor progression via an m6A-dependent epigenetic silencing of pre-miR-181b-1/YAP signaling axis in osteosarcoma, Cell Death Dis. 12 (1) (2021 Jan 11) 60, https://doi.org/10.1038/s41419-020-03315-x. PMID: 33431791; PMCID: PMC7801648.

[21] X. Qiu, S. Yang, S. Wang, J. Wu, B. Zheng, K. Wang, S. Shen, S. Jeong, Z. Li, Y. Zhu, T. Wu, X. Wu, R. Wu, W. Liu, H.Y. Wang, L. Chen, M6A demethylase ALKBH5 regulates PD-L1 expression and tumor immunoenvironment in intrahepatic cholangiocarcinoma, Cancer Res. 81 (18) (2021 Sep 15) 4778–4793, https://doi.org/10.1158/0008-5472.CAN-21-0468. Epub 2021 Jul 23. PMID: 34301762.

[22] J. Qu, H. Yan, Y. Hou, W. Cao, Y. Liu, E. Zhang, J. He, Z. Cai, RNA demethylase ALKBH5 in cancer: from mechanisms to therapeutic potential, J. Hematol. Oncol. 15 (1) (2022 Jan 21) 8, https://doi.org/10.1186/s13045-022-01224-4. PMID: 35063010; PMCID: PMC8780705.

[23] G. Li, R. Luo, W. Zhang, S. He, B. Wang, H. Liang, Y. Song, W. Ke, Y. Shi, X. Feng, K. Zhao, X. Wu, Y. Zhang, K. Wang, C. Yang, m6A hypomethylation of DNMT3B regulated by ALKBH5 promotes intervertebral disc degeneration via E4F1 deficiency, Clin. Transl. Med. 12 (3) (2022 Mar) e765, https://doi.org/10.1002/ctm2.765. Erratum in: Clin Transl Med. 2023 Aug;13(8):e1353. PMID: 35340126; PMCID: PMC8957938.

[24] X. Wang, L. Tian, Y. Li, J. Wang, B. Yan, L. Yang, Q. Li, R. Zhao, M. Liu, P. Wang, Y. Sun, RBM15 facilitates laryngeal squamous cell carcinoma progression by regulating TMBIM6 stability through IGF2BP3 dependent, J. Exp. Clin. Cancer Res. 40 (1) (2021 Feb 26) 80, https://doi.org/10.1186/s13046-021-01871-4. PMID: 33637103; PMCID: PMC7912894.

[25] P. Knuckles, T. Lence, I.U. Haussmann, D. Jacob, N. Kreim, S.H. Carl, I. Masiello, T. Hares, R. Villaseñor, D. Hess, M.A. Andrade-Navarro, M. Biggiogera, M. Helm, M. Soller, M. Bühler, J.Y. Roignant, Zc3h13/Flacc is required for adenosine methylation by bridging the mRNA-binding factor Rbm15/Spenito to the m6A machinery component Wtap/Fl(2)d, Genes Dev. 32 (5-6) (2018 Mar 1) 415–429, https://doi.org/10.1101/gad.309146.117. Epub 2018 Mar 13. PMID: 29535189; PMCID: PMC5900714.

[26] F. Yu, A.C. Zhu, S. Liu, B. Gao, Y. Wang, N. Khudaverdyan, C. Yu, Q. Wu, Y. Jiang, J. Song, L. Jin, C. He, Z. Qian, RBM33 is a unique m6A RNA-binding protein that regulates ALKBH5 demethylase activity and substrate selectivity, Mol. Cell 83 (12) (2023 Jun 15) 2003–2019.e6, https://doi.org/10.1016/j.molcel.2023.05.010. Epub 2023 May 30. PMID: 37257451; PMCID: PMC10330838.

[27] Y. Fang, X. Wu, Y. Gu, R. Shi, T. Yu, Y. Pan, J. Zhang, X. Jing, P. Ma, Y. Shu, LINC00659 cooperated with ALKBH5 to accelerate gastric cancer progression by stabilising JAK1 mRNA in an m6 A-YTHDF2-dependent manner, Clin. Transl. Med. 13 (3) (2023 Mar) e1205, https://doi.org/10.1002/ctm2.1205. PMID: 36864711; PMCID: PMC9982078.

[28] J.P. Kastan, M.W. Tremblay, M.C. Brown, J.D. Trimarco, E.Y. Dobrikova, M.I. Dobrikov, M. Gromeier, Enterovirus 2A(pro) cleavage of the YTHDF m(6)A readers implicates YTHDF3 as a mediator of type I interferon-driven JAK/STAT signaling, mBio 12 (2) (2021), https://doi.org/10.1128/mBio.00116-21.

[29] F. Zheng, F. Du, J. Zhao, X. Wang, Y. Si, P. Jin, H. Qian, B. Xu, P. Yuan, The emerging role of RNA N6-methyladenosine methylation in breast cancer, Biomark. Res. 9 (1) (2021 May 27) 39, https://doi.org/10.1186/s40364-021-00295-8. PMID: 34044876; PMCID: PMC8161983.

[30] Z. Zou, C. Sepich-Poore, X. Zhou, J. Wei, C. He, The mechanism underlying redundant functions of the YTHDF proteins, Genome Biol. 24 (1) (2023 Jan 24) 17, https://doi.org/10.1186/s13059-023-02862-8. PMID: 36694229; PMCID: PMC9872407.

[31] Z. Su, Y. Zhang, J. Cao, Y. Sun, Y. Cai, B. Zhang, L. He, Z. Zhang, J. Xie, Q. Meng, L. Luo, F. Li, J. Li, J. Zhang, X. Chen, A. Hong, Hyaluronic acid-FGF2-derived peptide bioconjugates for suppression of FGFR2 and AR simultaneously as an acne antagonist, J. Nanobiotechnol. 21 (1) (2023 Feb 17) 55, https://doi.org/10.1186/s12951-023-01812-7. PMID: 36803994; PMCID: PMC9938603.

[32] T. Xue, X. Liu, M. Zhang, E Q, S. Liu, M. Zou, Y. Li, Z. Ma, Y. Han, P. Thompson, X. Zhang, PADI2-Catalyzed MEK1 citrullination activates ERK1/2 and promotes IGF2BP1-mediated SOX2 mRNA stability in endometrial cancer, Adv. Sci. 8 (6) (2021) 2002831, https://doi.org/10.1002/advs.202002831.

[33] Y. Liu, Q. Guo, H. Yang, X.W. Zhang, N. Feng, J.K. Wang, T.T. Liu, K.W. Zeng, P.F. Tu, Allosteric regulation of IGF2BP1 as a novel strategy for the activation of tumor immune microenvironment, ACS Cent. Sci. 8 (8) (2022 Aug 24) 1102–1115, https://doi.org/10.1021/acscentsci.2c00107. Epub 2022 May 17. PMID: 36032766; PMCID: PMC9413439.

[34] I.A. Elcheva, T. Wood, K. Chiarolanzio, B. Chim, M. Wong, V. Singh, C.P. Gowda, Q. Lu, M. Hafner, S. Dovat, Z. Liu, S.A. Muljo, V.S. Spiegelman, RNA-binding protein IGF2BP1 maintains leukemia stem cell properties by regulating HOXB4, MYB, and ALDH1A1, Leukemia 34 (5) (2020 May) 1354–1363, https://doi.org/10.1038/s41375-019-0656-9. Epub 2019 Nov 25. PMID: 31768017; PMCID: PMC7196026.

[35] I.A. Elcheva, T. Wood, K. Chiarolanzio, B. Chim, M. Wong, V. Singh, C.P. Gowda, Q. Lu, M. Hafner, S. Dovat, Z. Liu, S.A. Muljo, V.S. Spiegelman, RNA-binding protein IGF2BP1 maintains leukemia stem cell properties by regulating HOXB4, MYB, and ALDH1A1, Leukemia 34 (5) (2020) 1354–1363, https://doi.org/10.1038/s41375-019-0656-9.

[36] X. Zhang, S. Zhang, X. Yan, Y. Shan, L. Liu, J. Zhou, Q. Kuang, M. Li, H. Long, W. Lai, m6A regulator-mediated RNA methylation modification patterns are involved in immune microenvironment regulation of periodontitis, J. Cell Mol. Med. 25 (7) (2021) 3634–3645, https://doi.org/10.1111/jcmm.16469.

[37] G. Sogkas, S. Hirsch, K.M. Olsson, J.B. Hinrichs, T. Thiele, T. Seeliger, T. Skripuletz, R.E. Schmidt, T. Witte, A. Jablonka, D. Ernst, Lung involvement in primary Sjögren's syndrome-an under-diagnosed entity, Front. Med. 7 (332) (2020), https://doi.org/10.3389/fmed.2020.00332.

[38] L. Li, J. He, L. Zhu, Y. Yang, Y. Jin, R. Jia, X. Liu, Y. Liu, X. Sun, Z. Li, The clinical relevance of IL-17-producing CD4+CD161+ cell and its subpopulations in primary Sjögren's syndrome, J. Immunol. Res. 2015 (2015) 307453, https://doi.org/10.1155/2015/307453.

[39] L.J. Howson, G. Napolitani, D. Shepherd, H. Ghadbane, P. Kurupati, L. Preciado-Llanes, M. Rei, H.C. Dobinson, M.M. Gibani, K.W.W. Teng, E.W. Newell, N. Veerapen, G.S. Besra, A.J. Pollard, V. Cerundolo, MAIT cell clonal expansion and TCR repertoire shaping in human volunteers challenged with Salmonella Paratyphi A, Nat. Commun. 9 (1) (2018) 253, https://doi.org/10.1038/s41467-017-02540-x.

[40] E.W. Meermeier, B.F. Laugel, A.K. Sewell, A.J. Corbett, J. Rossjohn, J. McCluskey, M.J. Harriff, T. Franks, M.C. Gold, D.M. Lewinsohn, Human TRAV1-2-negative MR1-restricted T cells detect S. pyogenes and alternatives to MAIT riboflavin-based antigens, Nat. Commun. 7 (2016) 12506, https://doi.org/10.1038/ncomms12506.

[41] J. Liu, B.T. Harada, C. He, Regulation of gene expression by N(6)-methyladenosine in cancer, Trends Cell Biol. 29 (6) (2019) 487–499, https://doi.org/10.1016/j.tcb.2019.02.008.

[42] Y. Wu, W. Zhao, Y. Liu, X. Tan, X. Li, Q. Zou, Z. Xiao, H. Xu, Y. Wang, X. Yang, Function of HNRNPC in breast cancer cells by controlling the dsRNA-induced interferon response, EMBO J. 37 (23) (2018), https://doi.org/10.15252/embj.201899017.

[43] D. Han, J. Liu, C. Chen, L. Dong, Y. Liu, R. Chang, X. Huang, Y. Liu, J. Wang, U. Dougherty, M.B. Bissonnette, B. Shen, R.R. Weichselbaum, M.M. Xu, C. He, Anti-tumour immunity controlled through mRNA m6A methylation and YTHDF1 in dendritic cells, Nature 566 (7743) (2019 Feb) 270–274, https://doi.org/10.1038/s41586-019-0916-x. Epub 2019 Feb 6. Erratum in: Nature. 2019 Apr;568(7751):E3. PMID: 30728504; PMCID: PMC6522227.

[44] Q. Gou, C. Dong, H. Xu, B. Khan, J. Jin, Q. Liu, J. Shi, Y. Hou, PD-L1 degradation pathway and immunotherapy for cancer, Cell Death Dis. 11 (11) (2020 Nov 6) 955, https://doi.org/10.1038/s41419-020-03140-2. PMID: 33159034; PMCID: PMC7648632.

[45] Y. Lin, X. Jin, Q. Nie, M. Chen, W. Guo, L. Chen, Y. Li, X. Chen, W. Zhang, H. Chen, M. Jiang, H. Xiao, J. Zhang, F. Fu, C. Wang, YTHDF3 facilitates triple-negative breast cancer progression and metastasis by stabilizing ZEB1 mRNA in an m6A-dependent manner, Ann. Transl. Med. 10 (2) (2022 Jan) 83, https://doi.org/10.21037/atm-21-6857. PMID: 35282088; PMCID: PMC8848410.

[46] A. Visvanathan, V. Patil, A. Arora, A.S. Hegde, A. Arivazhagan, V. Santosh, et al., Essential role of METTL3-mediated m(6)A modification in glioma stem-like cells maintenance and radioresistance, Oncogene 37 (4) (2018) 522–533, https://doi.org/10.1038/onc.2017.351.

[47] Q. Cui, H. Shi, P. Ye, L. Li, Q. Qu, G. Sun, et al., m(6)A RNA methylation regulates the self-renewal and tumorigenesis of glioblastoma stem cells, Cell Rep. 18 (11) (2017) 2622–2634, https://doi.org/10.1016/j.celrep.2017.02.059.

[48] H. Wang, B. Xu, J. Shi, N6-methyladenosine METTL3 promotes the breast cancer progression via targeting Bcl-2, Gene 722 (2020) 144076, https://doi.org/10.1016/j.gene.2019.144076.

[49] X. Cao, Q. Geng, D. Fan, Q. Wang, X. Wang, M. Zhang, L. Zhao, Y. Jiao, T. Deng, H. Liu, J. Zhou, L. Jia, C. Xiao, m6A methylation: a process reshaping the tumour immune microenvironment and regulating immune evasion, Mol. Cancer 22 (1) (2023 Mar 1) 42, https://doi.org/10.1186/s12943-022-01704-8. PMID: 36859310; PMCID: PMC9976403.
[50] G. Sogkas, S. Hirsch, K.M. Olsson, J.B. Hinrichs, T. Thiele, T. Seeliger, T. Skripuletz, R.E. Schmidt, T. Witte, A. Jablonka, D. Ernst, Lung involvement in primary Sjögren's syndrome-an under-diagnosed entity, Front. Med. 7 (332) (2020), https://doi.org/10.3389/fmed.2020.00332.
[51] L. Li, J. He, L. Zhu, Y. Yang, Y. Jin, R. Jia, X. Liu, Y. Liu, X. Sun, Z. Li, The clinical relevance of IL-17-producing CD4+CD161+ cell and its subpopulations in primary Sjögren's syndrome, J. Immunol. Res. 2015 (2015) 307453, https://doi.org/10.1155/2015/307453.
[52] L. Li, J. He, L. Zhu, Y. Yang, Y. Jin, R. Jia, X. Liu, Y. Liu, X. Sun, Z. Li, The clinical relevance of IL-17-producing CD4+CD161+ cell and its subpopulations in primary Sjögren's syndrome, J. Immunol. Res. 2015 (2015) 307453, https://doi.org/10.1155/2015/307453.
[53] I. Smets, T. Prezzemolo, M. Imbrechts, K. Mallants, T. Mitera, S. Humblet-Baron, B. Dubois, P. Matthys, A. Liston, A. Goris, Treatment-Induced BAFF expression and B cell biology in multiple sclerosis, Front. Immunol. 12 (2021) 676619, https://doi.org/10.3389/fimmu.2021.676619.
[54] M.J. Butcher, J. Zhu, Recent advances in understanding the Th1/Th2 effector choice, Facul. Rev. 10 (30) (2021), https://doi.org/10.12703/r/10-30.
[55] M. Paplinska-Goryca, P. Misiukiewicz-Stepien, M. Proboszcz, P. Nejman-Gryz, K. Gorska, R. Krenke, The expressions of TSLP, IL-33, and IL-17A in monocyte derived dendritic cells from asthma and COPD patients are related to epithelial-macrophage interactions, Cells 9 (9) (2020), https://doi.org/10.3390/cells9091944.
[56] W. Fei, Y. Hou, N. Yue, X. Zhou, Y. Wang, L. Wang, A. Li, J. Zhang, The effects of aqueous extract of Maca on energy metabolism and immunoregulation, Eur. J. Med. Res. 25 (1) (2020) 24, https://doi.org/10.1186/s40001-020-00420-7.
[57] P. Kiesler, A. Shakya, D. Tantin, D. Vercelli, An allergy-associated polymorphism in a novel regulatory element enhances IL13 expression, Hum. Mol. Genet. 18 (23) (2009) 4513–4520, https://doi.org/10.1093/hmg/ddp411.
[58] J.W. Williams, M.Y. Tjota, B.S. Clay, B. Vander Lugt, H.S. Bandukwala, C.L. Hrusch, D.C. Decker, K.M. Blaine, B.R. Fixsen, H. Singh, R. Sciammas, A.I. Sperling, Transcription factor IRF4 drives dendritic cells to promote Th2 differentiation, Nat. Commun. 4 (2990) (2013), https://doi.org/10.1038/ncomms3990.